Rice 7-Hydroxymethyl Chlorophyll *a* Reductase Is Involved in the Promotion of Chlorophyll Degradation and Modulates Cell Death Signaling

Weilan Piao[1], Su-Hyun Han[1], Yasuhito Sakuraba[1,2,*], and Nam-Chon Paek[1,*]

[1]Department of Plant Science, Plant Genomics and Breeding Institute, and Research Institute of Agriculture and Life Sciences, Seoul National University, Seoul 08826, Korea, [2]Present address: Graduate School of Agricultural and Life Sciences, Biotechnology Research Center, The University of Tokyo, Tokyo 113-8657, Japan
*Correspondence: sakuraba0425@gmail.com (YS); ncpaek@snu.ac.kr (NCP)
http://dx.doi.org/10.14348/molcells.2017.0127
www.molcells.org

The loss of green coloration via chlorophyll (Chl) degradation typically occurs during leaf senescence. To date, many Chl catabolic enzymes have been identified and shown to interact with light harvesting complex II to form a Chl degradation complex in senescing chloroplasts; this complex might metabolically channel phototoxic Chl catabolic intermediates to prevent oxidative damage to cells. The Chl catabolic enzyme 7-hydroxymethyl Chl *a* reductase (HCAR) converts 7-hydroxymethyl Chl *a* (7-HMC *a*) to Chl *a*. The rice (*Oryza sativa*) genome contains a single *HCAR* homolog (*OsHCAR*), but its exact role remains unknown. Here, we show that an *oshcar* knockout mutant exhibits persistent green leaves during both dark-induced and natural senescence, and accumulates 7-HMC *a* and pheophorbide *a* (Pheo *a*) in green leaf blades. Interestingly, both rice and Arabidopsis *hcar* mutants exhibit severe cell death at the vegetative stage; this cell death largely occurs in a light intensity-dependent manner. In addition, 7-HMC *a* treatment led to the generation of singlet oxygen ($^1O_2$) in Arabidopsis and rice protoplasts in the light. Under herbicide-induced oxidative stress conditions, leaf necrosis was more severe in *hcar* plants than in wild type, and *HCAR*-overexpressing plants were more tolerant to reactive oxygen species than wild type. Therefore, in addition to functioning in the conversion of 7-HMC *a* to Chl *a* in senescent leaves, HCAR may play a critical role in protecting plants from high light-induced damage by preventing the accumulation of 7-HMC *a* and Pheo *a* in developing and mature leaves at the vegetative stage.

INTRODUCTION

Leaf senescence is characterized by the gradual loss of green coloration, mainly due to chlorophyll (Chl) degradation. Since free Chl and its catabolic intermediates are highly phototoxic, they must be degraded rapidly and completely, along with photosynthetic proteins and other macromolecules. During this process, Chl is ultimately converted to non-phototoxic colorless catabolites, termed phyllobilins, through in the PAO/phyllobilin pathway (Hörtensteiner and Krautler, 2011); this reaction requires seven Chl catabolic enzymes (CCEs), which function in senescing chloroplasts (Hörtensteiner, 2013). Six CCE genes have been characterized in rice and/or Arabidopsis, including *NON-YELLOW COLORING1* (*NYC1*, Horie et al., 2009; Kusaba et al., 2007) and *NYC1-LIKE* (*NOL*, Horie et al., 2009; Sato et al., 2009), along with genes encoding Chl *b* reductases, 7-hydroxymethyl Chl *a* reductase (*HCAR*, Meguro et al., 2011), pheophytinase (*PPH*, Schelbert et al., 2009), pheophorbide *a* oxygenase (*PAO*,

Pružinská et al., 2003), and red Chl catabolite reductase (*RCCR*, Pružinská et al., 2007). Most mutants of these CCEs show a stay-green phenotype during natural senescence and/or artificially induced senescence, including dark- and phytohormone-induced leaf senescence, due to an impaired Chl degradation pathway (Horie et al., 2009; Hörtensteiner, 2009; Kusaba et al., 2007; Schelbert et al., 2009).

In addition to these CCEs, STAY-GREEN1 (SGR1, also termed NONYELLOWING1, NYE1) homologs have been isolated in various plant species, where they function as key positive regulators of Chl degradation; *sgr* mutants typically show a strong stay-green phenotype during both natural and dark-induced senescence (DIS) (Barry et al., 2008; Park et al., 2007; Ren et al., 2007; Sakuraba et al., 2015a). We previously showed that Arabidopsis SGR1/NYE1 physically interacts with the six CCEs and LHCII, forming a multi-protein complex that is likely important for rapid detoxification of Chl catabolic intermediates in senescing chloroplasts (Sakuraba et al., 2012; 2013).

In addition to SGR1, all plants contain an additional SGR subgroup, SGR-LIKE (SGRL). The C-terminal sequence of SGRL differs considerably from that of SGR (Hörtensteiner, 2009; Sakuraba et al., 2015a). *OsSGRL*-overexpressing plants show a premature leaf yellowing phenotype (Rong et al., 2013). Similarly, overexpression of *AtSGRL* accelerates leaf yellowing under abiotic stresses, including high salinity and heat stress, at the vegetative stage (Sakuraba et al., 2014b), indicating that SGRL mainly contributes to Chl degradation during vegetative growth. Very recently, Shimoda et al. (2016) reported that SGR and SGRL homologs have Mg-dechelatase activity for Chl *a* and chlorophyllide a, respectively, representing the last of the seven CCEs in the PAO/phyllobilin pathway.

Cell death is a common process that occurs in response to pathogen attack or abiotic environmental stress. Cell death, often referred to as the "hypersensitive response (HR)", has important functions in protecting plants from advancing pathogen infection (Greenberg et al., 1994). A few CCEs play an important role in inhibiting HR, because Chl catabolic intermediates act as strong photosensitizers in planta. Thus, some mutants of CCEs show an accelerated cell death phenotype. In Arabidopsis, *accelerated cell death1* (*acd1*) and *acd2* are null mutants of *PAO* and *RCCR*, respectively. Under normal photoperiodic growth conditions, *acd1* and *acd2* accumulate pheophorbide *a* (Pheo *a*) and RCC in their green leaves, respectively, causing excessive accumulation of reactive oxygen species (ROS). Consequently, *acd1* and *acd2* show a necrotic phenotype and growth retardation (Pružinská et al., 2003; 2007). Cell death symptoms were also observed in RNAi-mediated knockdown mutants of *PAO* and *RCCR* in rice (Tang et al., 2011). Interestingly, *RCCR*-overexpressing Arabidopsis plants exhibit increased tolerance to oxidative stress-induced cell death (Yao and Greenberg, 2006), indicating that some CCEs have the potential for controlling cell death mechanisms, possibly through the metabolic channeling of phototoxic Chl intermediates.

Arabidopsis HCAR, which catalyzes the reduction of 7-hydroxymethyl Chl *a* (7-HMC *a*) to Chl *a*, is a CCE that func-

tions in senescing chloroplasts (Meguro et al., 2011). HCAR is a homolog of cyanobacterial divinyl reductases, which participate in Chl biosynthesis (Ito et al., 2008). The Arabidopsis *hcar* (*athcar*) mutant shows a stay-green phenotype during DIS, accompanied by strong accumulation of 7-HMC *a* and Pheo *a* (Meguro et al., 2011). Furthermore, HCAR physically interacts with other CCEs, such as SGR1/NYE1, NYC1, NOL, RCCR, and LHCII, indicating that HCAR is a component of the Chl degradation complex (Sakuraba et al., 2013). The rice genome encodes a homolog of HCAR (hereafter OsHCAR, Supplementary Fig. S1), but its physiological role remains unknown.

In this study, we performed a functional analysis of *OsHCAR* using a T-DNA insertion knockout mutant. The *oshcar* mutant showed a stay-green phenotype during DIS, along with strong accumulation of the Chl catabolic intermediates 7-HMC *a* and Pheo *a*, indicating that OsHCAR is a component of the Chl degradation complex in rice. In addition, both the *oshcar* and *athcar* mutants showed an accelerated cell death phenotype due to excessive accumulation of singlet oxygen ($^1O_2$). Furthermore, 7-HMC *a*-treated protoplasts produced large amounts of $^1O_2$, indicating that rice and Arabidopsis HCAR play an important role in protecting pre-senescent leaf cells from cell death. We discuss the possible roles played by HCAR in Chl degradation and in protecting plants from cell death.

MATERIALS AND METHODS

Plant materials and growth conditions
The *oshcar* mutant and its parental wild-type *japonica* rice cultivar 'Hwayoung' were grown in a growth chamber under long days (LD, 14.5 h light, 30℃/9.5 h dark, 24℃, 300 μmol m^{-2} s^{-1}) or in a paddy field under natural LD (>14-h light/day) in Suwon, Korea (37°N latitude). The T-DNA insertion *oshcar* mutant (stock number: PFG_2A-00576) was obtained from the Crop Biotech Institute at Kyung Hee University, Korea (Jeon et al., 2000). For DIS, detached or attached leaves of 3-week-old plants were incubated in complete darkness. The *Arabidopsis thaliana* (*At*) T-DNA insertion *athcar* mutant (SALK_018790C) and the *AtHCAR*-overexpressing (*AtHCAR*-OX) line were described previously (Sakuraba et al., 2013), and they were grown under LD (16 h light/day, 70 μmol m^{-2} s^{-1}).

Plant transformation
To produce Arabidopsis lines ectopically expressing *OsHCAR*, pMDC43 harboring *35S:OsHCAR* was transformed into *Agrobacterium tumefaciens* stain GV3101. *Agrobacterium*-mediated transformation of the *athcar* mutant was performed using the floral-dip method (Zhang et al., 2006). Transformants were confirmed by genomic PCR using *OsHCAR*-specific primers (Supplementary Table 1).

Chl quantification
To measure total Chl concentrations, pigments were extracted from leaf tissues with 80% ice-cold acetone. Chl concentrations were determined by spectrophotometry, as described previously (Porra et al., 1989).

SDS-PAGE and immunoblot analysis

Total protein extracts were prepared from leaf tissues, using the middle section of the third leaf in the main culm of each 2-month-old rice plant grown under LD. Leaf tissues were ground in liquid nitrogen, and 10 mg aliquots were homogenized with 100 µl of sample buffer (50 mM Tris, pH 6.8, 2 mM EDTA, 10% glycerol, 2% SDS, and 6% 2-mercaptoethanol). The homogenates were centrifuged at 10,000 × g for 3 min, and the supernatants were denatured at 80℃ for 5 min. A 4 µl aliquot of each sample was subjected to 12% (w/v) SDS-PAGE, followed by electroblotting onto a Hybond-p membrane (GE Healthcare). Antibodies against photosystem proteins Lhca1, Lhca2, Lhcb1, Lhcb2, Lhcb4, Lhcb5, CP43, and PsaA (Agrisera, Sweden) were used for immunoblot analysis, and RbcL was visualized by Coomassie Brilliant Blue (CBB) staining. The level of each protein was examined using the ECL system with WESTSAVE (AbFRONTIER, Korea) according to the manufacturer's protocol.

Measurement of *Fv/Fm* ratios

The *Fv/Fm* ratios of wild type and *oshcar* plants grown in the paddy field were measured using an OS-30p instrument (OptiSciences, USA), as previously described (Sakuraba et al., 2015b). The middle section of each flag leaf was adapted in the dark for 5 min to complete oxidation of QA. After dark treatment, the *Fv/Fm* ratio was measured in the paddy field. For both experiments, more than three experimental replicates per plant were conducted.

RNA isolation and quantitative reverse-transcription PCR (qPCR) analysis

For the RT reactions, total RNA was extracted from rice leaf blades and other tissues using an RNA Extraction Kit (Macrogen, Korea). First-strand cDNA was prepared with 2 µg total RNA using M-MLV reverse transcriptase and oligo(dT)$_{15}$ primer (Promega) in a total volume of 25 µl and diluted with 75 µl water. For quantitative reverse-transcription PCR (qPCR), a 20 ml mixture was prepared including first-strand cDNA equivalent to 2 µl total RNA, 10 µl 2× GoTaq master mix (Promega), 6 µl distilled water, and gene-specific forward and reverse primers (Supplementary Table 1). The qPCR was performed using a LightCycler 480 (Roche Diagnostics). Rice *Ubiquitin5* (*UBQ5*) or *GAPDH* (encoding glyceraldehyde phosphate dehydrogenase) was used as an internal control. The relative expression level of each gene was calculated using the $2^{-\Delta\Delta CT}$ method, as previously described (Livak and Schmittgen, 2001).

HPLC analysis

Leaves were weighed and pulverized in acetone using a Shake Master grinding apparatus (BioMedical Science), and the extracts were centrifuged for 15 min at 22,000 × g. The pigments were separated on a Symmetry C8 column (150 × 4.6 mm; Waters) as described previously (Zapata et al., 2000). The elution profiles were monitored by measuring the absorbance at 653 nm (SPD-M10A; Shimadzu), and pigments were identified based on their retention times and spectral patterns. Pigment quantification was performed based on the areas of the peaks.

Reactive oxygen species detection

For singlet oxygen ($^1O_2$) detection, Singlet Oxygen Sensor Green (SOSG; Invitrogen) reagent was used, as previously described (Han et al., 2012). Leaves of 2-week-old plants were treated with 50 mM SOSG in 10 mM sodium phosphate buffer (pH 7.5). After 30 min incubation, fluorescence emission following excitation at 480 nm was imaged using a laser scanning confocal microscope (LSM510, Carl Zeiss-LSM510). The red autofluorescence from Chl was also detected following excitation at 543 nm. Detection of hydrogen peroxide (H_2O_2) and superoxide (O_2^-) was carried out as previously described (Li et al., 2010), with minor modifications. Hydrogen peroxide (H_2O_2) and superoxide (O_2^-) were detected using 3,3-diaminobendizine (DAB) and nitroblue tetrazolium chloride (NBT), respectively. Leaves of 2-month-old plants grown in a paddy field were sampled and incubated in 0.1% DAB (Sigma) or 0.05% NBT (Duchefa) in 50 mM sodium phosphate buffer (pH 7.5) at room temperature overnight with gentle shaking. Chlorophyll was completely removed by incubation in 90% ethanol at 80℃.

Yeast two-hybrid analysis

The full-length cDNAs of rice *HCAR*, *SGR*, *NYC1*, *NOL*, *PPH*, *PAO*, and *RCCR* in entry vectors were inserted into destination vectors pDEST32 (bait) and pDEST22 (prey) (Invitrogen). Yeast strain MaV203 was used for cotransformation of bait and prey clones, and β-galactosidase activity was measured via a liquid assay using chlorophenol red-β-D-galactoside (Roche Applied Science) according to the Yeast Protocols Handbook (Clontech).

Trypan blue staining

Trypan blue staining was performed as described by Koch and Slusarenko (1990) with minor modifications. Arabidopsis leaves and rice leaf discs exposed to herbicide-induced oxidative stress were incubated overnight in lactophenol-trypan blue solution (10 ml lactic acid, 10 ml glycerol, 10 g phenol, and 10 mg trypan blue dissolved in 10 ml distilled water). The stained leaves were boiled for 1 min and decolorized in 60% glycerol solution.

Oxidative stress assay

For MV treatment, one-month-old rice plants were sprayed with 50 µM methyl viologen dichloride (MV, Sigma), and three-week-old Arabidopsis plants were sprayed with 10 µM MV. The plants were incubated under continuous light conditions for the indicated times.

Protoplast isolation and light treatment

Rice leaf protoplasts were isolated from 15- to 20-d-old plants as described previously (Liang et al., 2003). Arabidopsis protoplasts were isolated from 3-week-old rosette leaves as described previously (Wu et al., 2009). The protoplasts were resuspended with protoplast incubation solution (500 mM manntiol, 20 mM KCl, 4 mM MES [pH5.8]), and incubated in the dark (control), under moderate light (200 µmol m^{-2} s^{-1}), or under high light (500 µmol m^{-2} s^{-1}), without or with 10 µM Chl *b* (Sigma-Aldrich), Pheo *a* (Sigma-Aldrich), and 7-HMC *a*, at 22℃ under fluorescent light. $^1O_2$ produc-

tion in the protoplasts was visualized using singlet oxygen sensor green (SOSG, Invitrogen), and green fluorescence was observed under a Confocal Laser Scanning Microscope II (LSM710, Carl Zeiss).

RESULTS

Rice *hcar* mutants exhibit a stay-green phenotype during leaf senescence

The *Oryza sativa* genome contains only a single *HCAR* homolog (*OsHCAR*, LOC_Os04g25400), and the amino acid sequence of OsHCAR is highly similar to those of HCAR homologs in other plant species (Supplementary Fig. 1). To elucidate the function of HCAR in leaf senescence in rice, we obtained the T-DNA insertion line PFG_2A-00576, which

contains a single T-DNA fragment inserted into the fifth exon of *HCAR* (Fig. 1A) and does not accumulate *HCAR* transcripts in senescing leaves (Fig. 1B), indicating that this mutant harbors a knockout allele of *HCAR* (hereafter *oshcar*).

Like most CCE mutants in Arabidopsis, *athcar* mutants show a stay-green phenotype during DIS (Meguro et al., 2011; Sakuraba et al., 2013). Thus, we examined the phenotype of the *oshcar* mutant during DIS. At the vegetative stage, the leaf color of *oshcar* was almost the same as that of wild type. However, the entire plant showed a stay-green phenotype after 14 days of dark incubation (14 DDI; Fig. 1C). We also confirmed that detached leaf segments of *oshcar* also showed stay-green phenotype after 6 DDI (Fig. 1D). The stay-green phenotype was observed in the *OsHCAR/oshcar* heterozygous progenies that were segregated from the
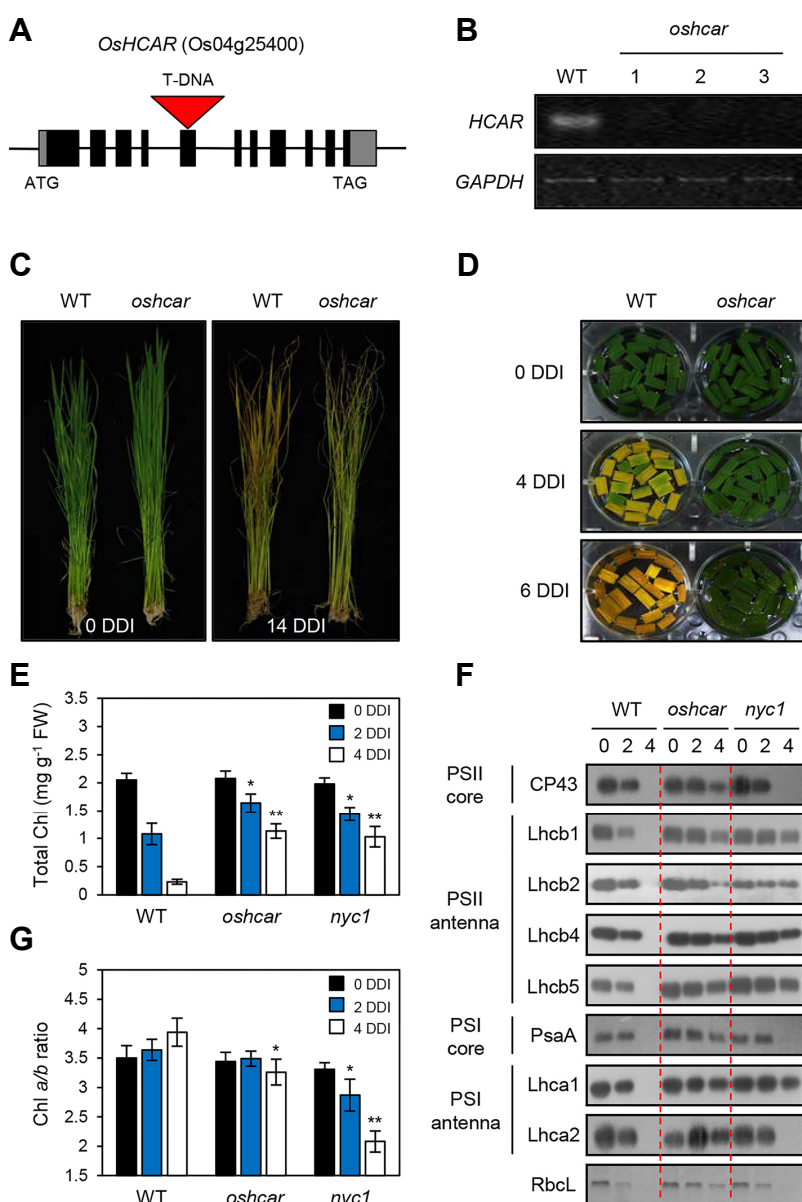

Fig. 1. Green leaf color persists much longer during DIS in the *hcar* mutant than in wild type. (A) The T-DNA insertion in the tenth exon of *HCAR* in Korean *japonica* rice cultivar 'Dongjin'. (B) The absence of *HCAR* transcripts in the *hcar* mutant was confirmed by RT-PCR. Total RNA was extracted from the second leaf blades of one-month-old plants. *GAPDH* was used as an internal control. (C) Whole wild-type (WT) and *hcar* plants grown for one month under LD (14 h light/day) were transferred to darkness at 28℃ for 14 days (10 DDI). (D-G) Changes in color (D), total Chl level (E), photosystem protein level (F), and Chl *a/b* ratio (G) in WT and *hcar* leaf discs during dark incubation. Leaves from *nyc1* were used as a stay-green control. The leaf discs were incubated in 3 mM MES (pH 5.8) buffer abaxial side-up at 28℃ in darkness and sampled at different DDI for each experiment. (F) Antibodies against PSII antenna proteins (Lhcb1, Lhcb2, Lhcb4, and Lhcb5), PSI antenna proteins (Lhca1 and Lhca2), PSII core proteins (CP43), and PSI core protein (PsaA) were used for immunoblot analysis. RbcL proteins were visualized by Coomassie Brilliant Blue staining. (E, G) Mean and SD values were obtained from more than three biological samples. Asterisks indicate significant difference compared to WT (Student's *t*-test, *P < 0.05, **P < 0.01). DDI, day(s) of dark incubation.

T-DNA heterozygous (*OsHCAR/oshcar*) plants, similar to the *oshcar* homozygous progenies (Supplementary Fig. 2). We used detached leaf segments for further phenotypic characterization. To characterize the photosynthetic parameters in the mutant, we compared *oshcar* with a nonfunctional stay-green mutant, *nyc1*, which is impaired in Chl *b* reductase activity (Kusaba et al., 2007). Consistent with its visible phenotype, Chl was highly retained in *hcar* during DIS (Fig. 1E). We also investigated the levels of photosystem proteins during DIS. As shown in Fig. 1F, only LHC proteins, such as Lhcb1, Lhcb2, Lhcb4, Lhcb5, and Lhca1, were highly retained in the *nyc1* mutant, whereas all types of photosystem proteins were highly retained in the *oshcar* mutant after dark incubation (2 and 4 DDI), when all photosystem proteins were undetectable in wild type. Similarly, the Chl *a/b* ratios were unchanged in *oshcar* (Fig. 1G), while *nyc1* retained more Chl *b*, primarily in senescing leaves. In this study, we used the *oshcar* T3 seeds that were harvested in 2014. In addition, we also confirmed that T4 and T5 generations of *oshcar* mutants (harvested in 2015 and 2016, respectively) showed stay-green phenotype with highly retaining of Chl (Supplementary Fig. 3).
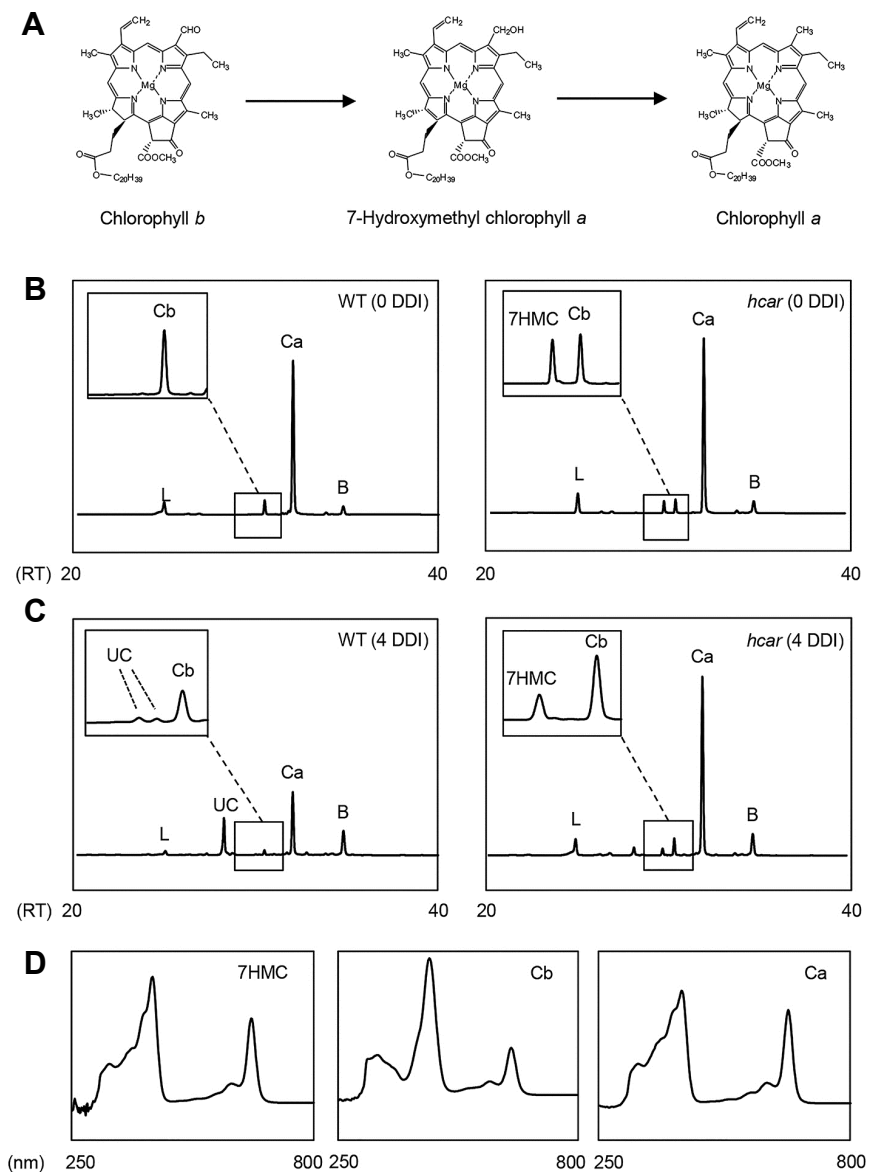

Fig. 2. Accumulation of 7-HMC *a* in the rice *hcar* mutant. (A) Chl *b* (Cb) is converted to 7-HMC *a* (7HMC) by Chl b reductase, which is then converted to Chl *a* (Ca) by HCAR. (B-D) HPLC profiles of Chls and 7-HMC *a* in WT and *hcar* leaves before (B) and after 4 DDI (C). Pigments were extracted from the leaves of one-month-old WT and *hcar* plants. (D) The identity of 7-HMC *a*, Chl *a*, and Chl *b* was confirmed by fluorescence spectroscopy from 250 to 800 nm. L, lutein; UC, unknown carotenoid; B, β-carotene. DDI, day(s) of dark incubation.

We then examined the senescence phenotype of *oshcar* during natural senescence. To this end, we grew the plants in a paddy field under natural LD conditions (~14 h light/day at 37° N latitude, Suwon, Korea). During grain filling, *oshcar* exhibited delayed senescence (Supplementary Fig. 4A) while retaining higher levels of Chl (Supplementary Fig. 4B) than wild type, as well as a high *Fv/Fm* ratio (Supplementary Fig. 4C), indicating that rice HCAR is involved in Chl degradation during both DIS and natural senescence. Some stay-green rice plants exhibit increased crop yields (Liang et al., 2014; Sakuraba et al., 2015b). Therefore, we measured several agronomic traits in the *oshcar* mutant, such as panicle length, plant height, number of grains per panicle, grain weight, and fertility. These traits were significantly lower in the *oshcar* mutant than in wild type (Supplementary Fig. 5), indicating that the stay-green trait of *oshcar* does not lead to increased grain yields.

To examine whether *OsHCAR* could recover the defects in the *athcar* mutant, we developed transgenic plants overexpressing *OsHCAR* in the *athcar* background (*35S:OsHCAR/athcar*). We evaluated the expression of *OsHCAR* in three independent transgenic lines by RT-PCR (Supplementary Fig. 6A). The *athcar* mutant stayed green after dark treatment, as previously reported (Meguro et al., 2011); in contrast, plants from the three transgenic lines senesced normally during dark treatment (Supplementary Figs. 6B and 6C), indicating that the role of HCAR in Chl degradation is conserved between Arabidopsis and rice.

Rice HCAR is enzymatically equivalent to Arabidopsis HCAR

HCAR is a CCE that converts 7-HMC *a* to Chl *a* (Fig. 2A). In Arabidopsis, 7-HMC *a* accumulates in the *hcar* mutant, although it is detected only under DIS conditions (Meguro et al., 2011). To examine whether 7-HMC *a* accumulates in the *oshcar* mutant, we performed HPLC analysis. Chl and its intermediates were extracted from green leaves (0 DDI) and dark-treated leaves (5 DDI) from wild type and *oshcar* plants. The substrate of HCAR, 7-HMC *a*, was undetectable in wild-type leaves, but it accumulated to levels high enough to detect in *hcar* leaves before and after dark treatment (Figs. 2B and 2C), which also occurs in the *athcar* mutant (Supplementary Fig. 7; Meguro et al., 2011), indicating that HCAR is also essential for the reduction of 7-HMC *a* to Chl *a* in rice.

We previously used yeast two-hybrid and co-immunoprecipitation assays to show that in Arabidopsis, HCAR physically interacts with other CCEs (SGR1/NYE1, NYC1, NOL, PPH, PAO, and RCCR), directly or indirectly, at LHCII (Sakuraba et al., 2013). Thus, it is highly likely that HCAR also interacts with other CCEs in rice. To investigate this notion, we performed yeast two-hybrid assays to examine the pairwise interactions between HCAR and six CCEs (SGR, NYC1, NOL, PPH, PAO, and RCCR). HCAR interacted with five CCEs, whereas PPH failed to interact with HCAR (Fig. 3). Interestingly, HCAR interacted with itself, suggesting that it may form dimers that interact with other CCEs at LHCII and induce Chl degradation.
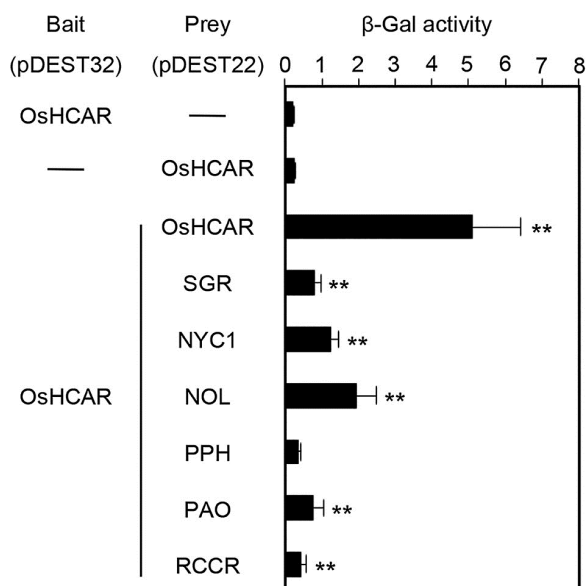

Fig. 3. Rice HCAR directly interacts with other CCEs in yeast two-hybrid assays. Rice HCAR was cloned into bait vector pDEST32, and HCAR, SGR, NYC1, NOL, PPH, PAO, and RCCR genes were cloned into prey vector pDEST22. Relative β-galactosidase (β-Gal) activity was determined via liquid assays using chlorophenol red-β-D-galactoside (CPRG) as a substrate. Empty bait plasmids (-) were used as a negative control. Mean and SD values were obtained from five independent colonies. Asterisks indicate significant difference compared to the negative controls (Student's *t*-test, *P < 0.05, **P < 0.01).

The expression pattern of *OsHCAR* differs from that of *AtHCAR* during leaf senescence

To investigate how *HCAR* transcription is regulated in rice, we used RT-qPCR to examine the expression levels of *HCAR* in different tissues, including root, leaf sheath, leaf blade, tiller, tiller base, and internode tissue. *HCAR* mRNA was highly abundant in leaf sheath, leaf blade, and internode tissue, which contain Chls (Supplementary Fig. 8), indicating that like *AtHCAR*, *HCAR* plays an important role in green tissues in rice.

We next examined whether *HCAR* expression is altered during leaf senescence. During DIS, the mRNA levels of *HCAR* and six other CCE genes (*SGR*, *NYC1*, *NOL*, *PAO*, *PPH*, and *RCCR*) significantly increased during DIS (Fig. 4A). Interestingly, the expression pattern of *OsHCAR* was completely different from that of *AtHCAR*, which exhibits a rapid decrease in expression during senescence (Sakuraba et al., 2013). Similarly, during natural senescence, *HCAR* was expressed at high levels in the yellowing sector of the rice leaf blade (region 'd') but at significantly lower levels in the green sector (regions 'a' and 'b') (Fig. 4B), suggesting that the requirement phase of HCAR activity during leaf senescence in rice does somehow differ from that in Arabidopsis.
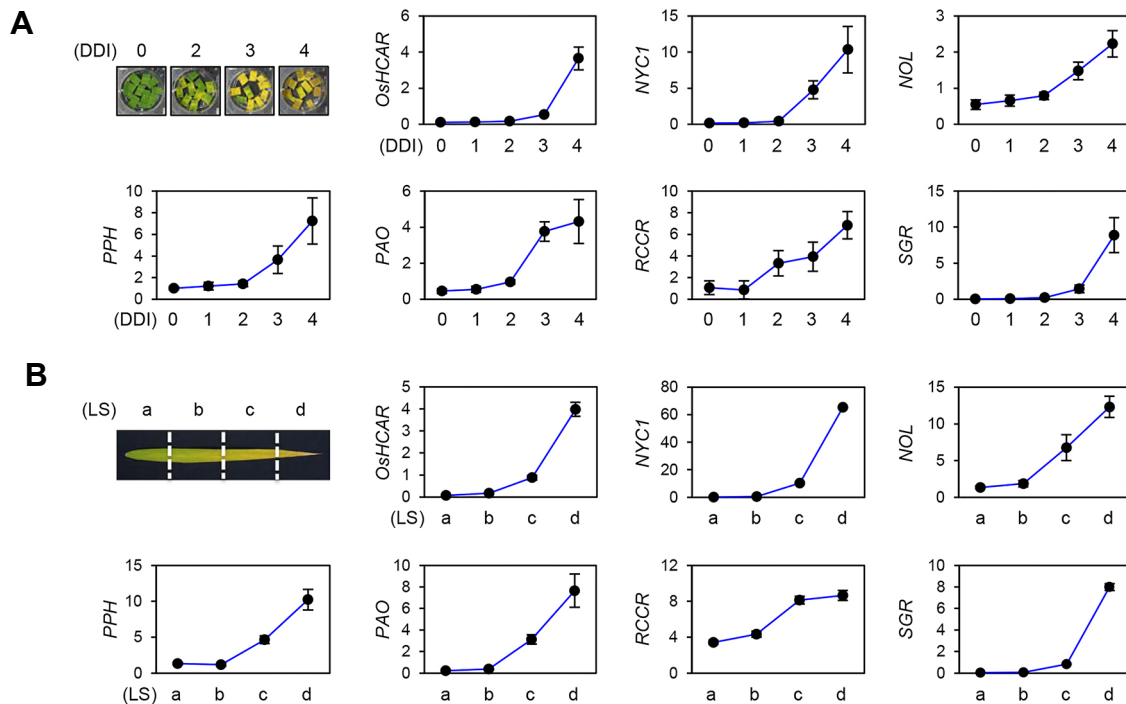
Fig. 4. Expression patterns of rice CCE genes during dark-induced and natural senescence. Expression of rice *HCAR, NYC1, NOL, PPH, PAO, RCCR,* and *SGR* during dark-induced (A) and natural senescence (B) was examined using the second leaf blades in the main culms of 70- and 120-d-old WT (Dongjin) plants, respectively. The relative expression levels were determined by RT-qPCR analysis and normalized to *UBQ5* transcript levels. Mean and SD values were obtained from more than three biological replicates. DDI, day(s) of dark incubation; LS, leaf sector.

Cell death occurs in *hcar* leaves during vegetative growth

In both Arabidopsis and rice, knockout and/or knockdown mutants of *PAO* and *RCCR* show an accelerated cell death phenotype, even under normal growth conditions, due to excess accumulation of phototoxic Chl intermediates (Pružinská et al., 2003, 2007; Tang et al., 2011). Thus, it is possible that HCAR is involved in regulating cell death signaling by modulating the metabolic processes underlying Chl degradation.

At 80 d after seeding (DAS) in the paddy field, the *oshcar* mutant exhibited accelerated cell death, especially in the tip sectors of older leaves (Figs. 5A-5C). In addition, under long-day (LD) conditions in growth chambers, the *oshcar* mutant showed accelerated cell death symptoms under high light, while cell death was barely detectable under low light (Supplementary Fig. 9), indicating that the cell death phenotype in *oshcar* leaves is largely dependent on light intensity. Because variegation or accelerated cell death symptoms in rice leaves are closely associated with ROS accumulation (Han et al., 2012; Li et al., 2010; Wang et al., 2015), we measured the levels of three types of ROS, i.e., singlet oxygen ($^1O_2$), hydrogen peroxide (H_2O_2), and superoxide (O_2^-), in *oshcar* leaves. We measured $^1O_2$ levels using Singlet Oxygen Sensor Green (SOSG), finding that SOSG signals were present in *oshcar* leaves but not in wild-type leaves (Fig. 5D). Similarly, H_2O_2 and O_2^- levels, based on the intensity of DAB and NBT staining, respectively, were much higher in *oshcar* leaves

than in wild-type leaves, primarily in older leaves (Figs. 5E and 5F). We then investigated whether cell death signaling-related genes are differentially expressed in *oshcar*. Genes that are upregulated during cell death, such as *JAmyb, Os-NAC4,* and *OsAPX1* (Han et al., 2012), were significantly upregulated in *hcar* leaves versus wild type, especially under high light (Supplementary Fig. 10). Taken together, these results indicate that *HCAR* plays an important role in the regulation of cell death in rice, as do *PAO* and *RCCR* (Tang et al., 2011).

The rice *hcar* mutant is susceptible to oxidative stress-induced cell death

It has previously been reported that the *atrccr* mutant, also known as *acd2*, is highly susceptible, whereas *AtRCCR*-OX plants are more tolerant to the treatment of methyl viologen, which induces oxidative stress by blocking the electron transport during photosynthesis in the chloroplast (Yao and Greenberg, 2006). To investigate whether the *oshcar* mutant also shows increased susceptibility to oxidative stress, we treated mutant and wild-type seedlings with 50 μM methyl viologen (MV). As expected, after 6 d of MV treatment, *oshcar* seedlings wilted much more quickly than WT (Figs. 6A and 6B). This leaf necrosis phenotype was also confirmed in *oshcar* heterozygous lines, while WT segregates did not show the phenotype, similar to Hwayoung WT (Supplementary Fig. 11). Cell death in the *oshcar* mutant was confirmed
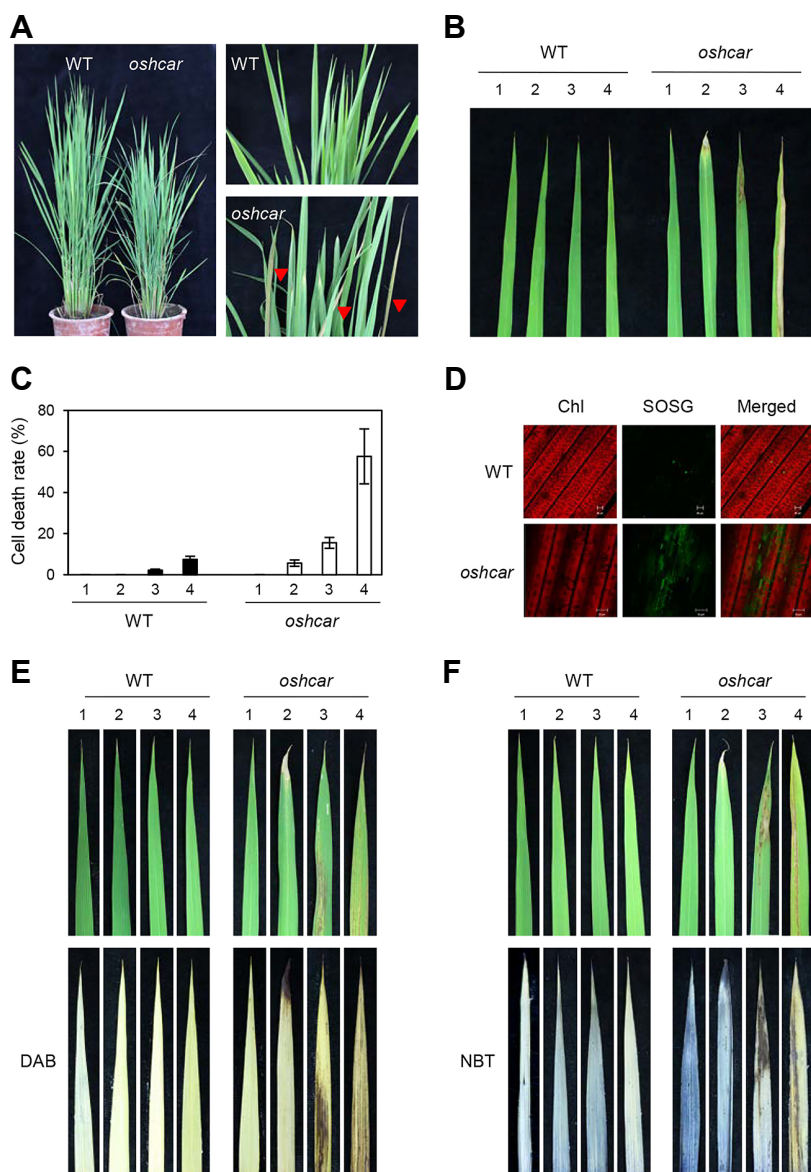
Fig. 5. The rice *hcar* mutant shows cell death symptoms in mature leaves. (A) Phenotypes of WT and *hcar* plants at 80 d after sowing (DAS) in the paddy field. (b, c) Phenotypes (B) and cell death rates (C) in leaf blades from WT and *hcar* plants shown in (a). Cell-death rate was calculated by the percentage of leaves in which more than 80% of leaf area became necrosis. 1, first (youngest); 2, second; 3, third; 4, fourth leaf blades from the top. (D) Singlet oxygen ($^1O_2$) accumulation in the third leaf blades of 80 DAS WT and *hcar* plants. $^1O_2$ was detected using Singlet Oxygen Sensor Green (SOSG) reagent. (E, F) Hydrogen peroxide (H_2O_2) and superoxide anion radicals (O_2^-) in the leaf blades of 80 DAS WT and *hcar* plants. The accumulation of H_2O_2 and O_2^- was visualized by staining with DAB (E) and NBT (F), respectively. DAB, 3,3-diaminobendizine; NBT, nitroblue tetrazolium chloride.

by trypan blue staining (Fig. 6C) and by the observation that the ion leakage rate in the mutants was higher than that of wild type (Fig. 6D). Moreover, high levels of $^1O_2$ accumulated in *oshcar* leaves during MV treatment (Fig. 6D), which also occurred in variegated *oshcar* leaves in the paddy field (Fig. 4).

Arabidopsis *HCAR* is involved in cell death signaling

Whereas the *oshcar* mutant showed accelerated cell death symptoms in both the paddy field and growth chamber (Figs. 5 and 6), this phenotype has not been reported for the *athcar* mutant, as previous studies of this mutant have mainly focused on its senescence phenotype during DIS (Meguro et al., 2011; Sakuraba et al., 2013). We therefore examined whether cell death occurs in *athcar* under normal conditions. Like *oshcar*, the 4-week-old *athcar* plants showed an accel-

erated cell death phenotype when grown under normal light (100 µmol m^{-2} s^{-1}) conditions (Fig. 7A), which was confirmed by trypan blue staining (Fig. 7B). Under high light (500 µmol m^{-2} s^{-1}) conditions, the cell death phenotype was more severe in *athcar* than in wild type and was observed even in 3-week-old plants (Figs. 7A and 7C). Furthermore, *athcar* plants were clearly smaller than wild-type plants (Fig. 7A), probably because severe cell death inhibits vegetative growth.

We then examined whether the *athcar* mutant is also highly susceptible to MV-induced oxidative stress. At 3 d after MV treatment, 4-week-old *athcar* plants displayed more severe cell death symptoms than wild type, whereas *AtHCAR*-OX plants were more tolerant to this treatment than wild type (Figs. 7D and 7E). The *athcar* mutant was also highly susceptible to oxyfluorfen-induced oxidative stress
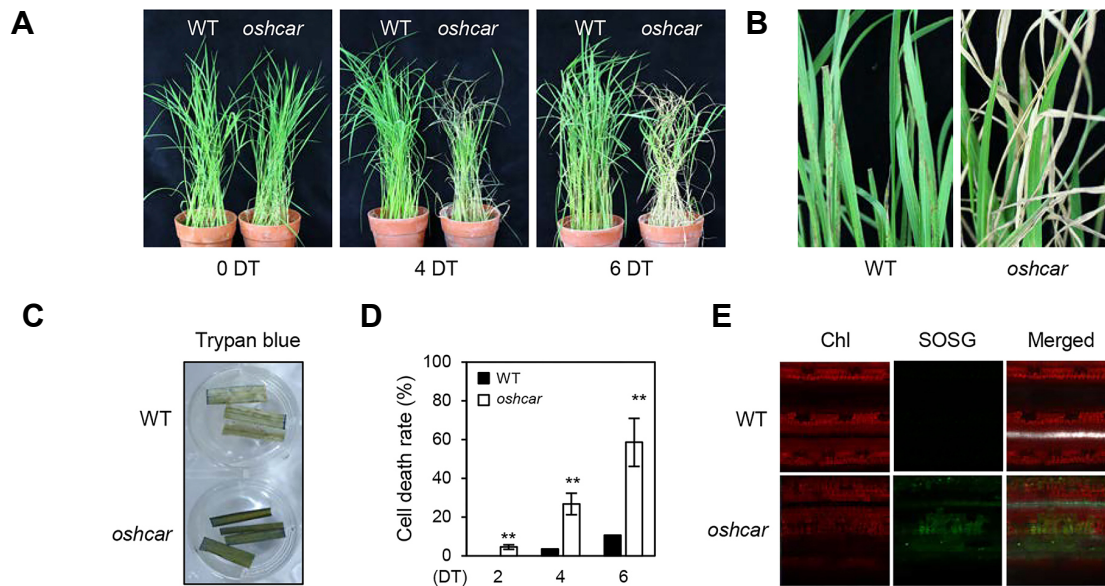
Fig. 6. The rice *hcar* mutant is susceptible to herbicide-induced cell death. (A) Phenotype of one-month-old WT and *hcar* plants during methyl viologen (MV, 50 µM) treatment. Phenotypes at 0, 4, and 6 days of MV treatment (DT) are shown, respectively. (B) Magnified image of WT and *hcar* leaves at 6 DT shown in (A). (C) Cell death in *hcar* leaves during MV treatment was confirmed by trypan-blue staining. (D) Cell death rates of WT and *hcar* plants during MV treatment. Black and white bars indicate WT and *hcar*, respectively. Cell-death rate was calculated by the percentage of leaves in which more than 80% of leaf area became necrosis. Asterisks indicate significant difference compared to WT (Student's *t*-test, *P < 0.05, **P < 0.01). (E) Singlet oxygen ($^1O_2$) accumulation in the second leaf blades of WT and *hcar* at 4 DT. Chl, chlorophyll; SOSG, singlet oxygen sensor green reagent.
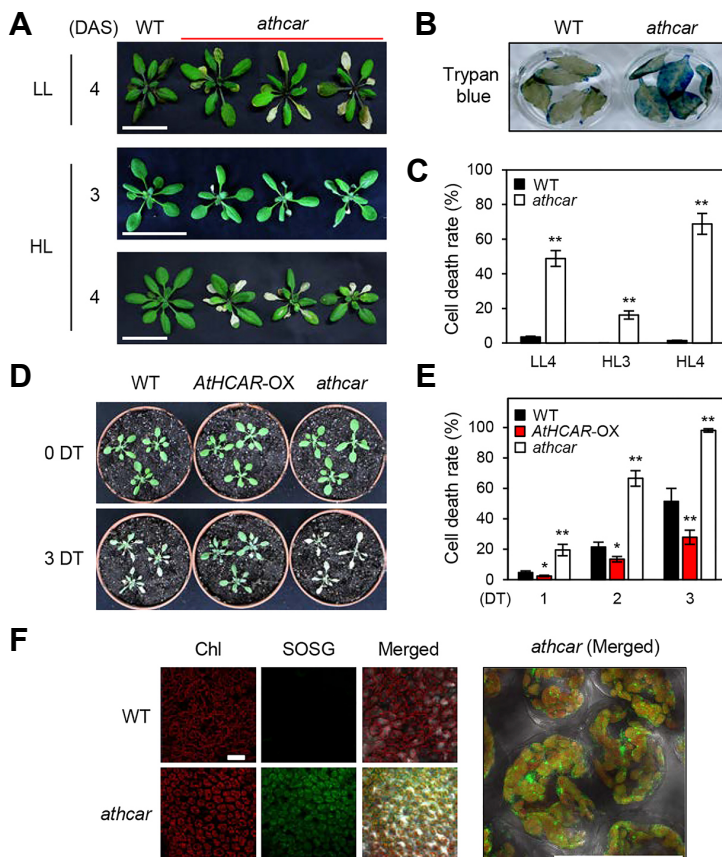

Fig. 7. Overexpression of *AtHCAR* increases tolerance to herbicide-induced cell death in Arabidopsis. (A) Phenotypes of 4-week-old WT and *athcar* plants grown under low light (LL) conditions (80 µmol m^{-2} s^{-1}, upper panel), and 3- and 4-week-old WT and *athcar* plants grown under high light (HL) conditions (300 µmol m^{-2} s^{-1}, lower panels). (B) Cell death in the fourth or fifth rosette leaves of 4-week-old WT and *athcar* plants grown under LL conditions visualized by trypan blue staining. (C) Cell death rate in the third and fourth leaves under the conditions described in (A). (D, E) Phenotypes (D) and cell death rates (E) of 3-week-old WT, *AtHCAR*-OX, and *athcar* plants under MV (10 µM) treatment. (F) Singlet oxygen ($^1O_2$) accumulation in the fourth leaves of WT and *athcar* plants after 1 day of MV treatment (1 DT). (C, E) Cell-death rate was calculated by the percentage of leaves that became completely necrotic. Asterisks indicate significant difference compared to WT (Student's *t*-test, *P < 0.05, **P < 0.01). DT, day(s) of MV treatment; SOSG, singlet oxygen sensor green reagent.
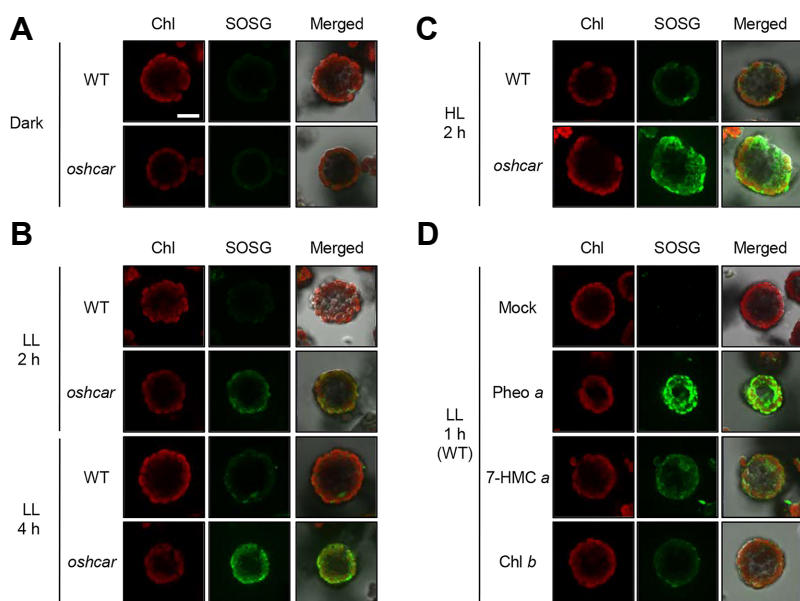
Fig. 8. 7-HMC *a* treatment induces $^1O_2$ production in rice protoplasts. Ten-day-old etiolated WT and *hcar* rice seedlings were irradiated for 15 h and used for protoplast isolation. (A-C) (A) WT and *hcar* protoplasts incubated in darkness (negative control), (B) under low light (LL; 50 μmol m^{-2} s^{-1}) for 2 h (upper panels) and 4 h (lower panels), and (C) under high light (HL; 200 μmol m^{-2} s^{-1}) for 2 h. (D) WT protoplasts were combined with 20 μM Pheo *a*, 7-HMC *a*, and Chl *b* and incubated under LL for 1 h. SOSG, singlet oxygen sensor green reagent.

(Supplementary Fig. 12). The hypersensitivity of *athcar* to MV-induced oxidative stress was further confirmed at a younger stage, i.e., one-week-old seedlings (Supplementary Fig. 13). Similar to *oshcar* leaves (Fig. 5), the MV-treated *athcar* leaves also accumulated high levels of singlet oxygen (Figs. 7F and 7G).

We then subjected *35S:OsHCAR/athcar* plants to MV-induced oxidative stress, finding that they were more tolerant of this stress than wild type (Supplementary Fig. 14), as were *AtHCAR*-OX plants, indicating that rice and Arabidopsis HCAR proteins play similar roles in regulating the oxidative stress response and cell death.

The production of singlet oxygen in *hcar* mutant protoplasts is caused by the accumulation of 7-HMC *a* and Pheo *a*

To analyze the role of HCAR in the cell death response in more detail, we monitored the production of singlet oxygen in protoplasts from wild-type and *oshcar* plants in rice. In the dark, neither wild-type nor *oshcar* protoplasts produced $^1O_2$ (Fig. 8A). After 2 h of low-light treatment, however, we detected green fluorescence corresponding to $^1O_2$ accumulation in wild-type protoplasts (Fig. 8B). Furthermore, we detected a much stronger fluorescence in *oshcar* protoplasts that were incubated for a longer period of time under low light (Fig. 8B). However, green fluorescence was barely detected in wild-type protoplasts under high light (Figs. 8B and 8C), indicating that *oshcar* protoplasts produce $^1O_2$ in a light-dependent manner. To examine whether the accumulation of 7-HMC *a* leads to $^1O_2$ production in *oshcar* protoplasts, we purified 7-HMC *a* from Chl *b* (Supplementary Fig. 15) and combined it with protoplasts from wild-type leaves. After 1 h of incubation under low light, we detected green fluorescence, although the fluorescence intensity was weaker compared with protoplasts incubated with Pheo *a*. In both cases, the fluorescence could be mainly observed at the
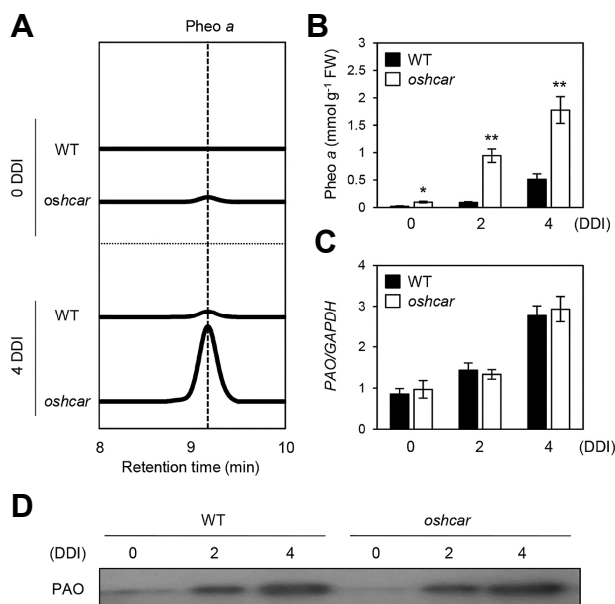

Fig. 9. Pheo *a* accumulates in the rice *hcar* mutant during DIS. (A, B) HPLC profiles (A) and quantification (B) of Pheo *a* in WT and *hcar* leaves before (0 DDI) and after 4 DDI. (C) *PAO* transcript levels in WT and *oshcar* leaves during dark incubation were determined by RT-qPCR analysis and normalized to *GAPDH* transcript levels. (D) PAO protein levels in WT and *hcar* leaves during DIS determined by immunoblot analysis using an anti-PAO antibody. (B, C) Black and white bars indicate WT and *hcar*, respectively. Mean and SD values were obtained from more than three biological replicates. DDI, day(s) of dark incubation.

outside of chloroplasts (probably at the outer membranes of chloroplasts and mitochondria), although a small portion of

signal can be seen in the chloroplasts. The addition of Chl *b* hardly increase $^1O_2$ accumulation (Fig. 8D). We obtained similar results using wild type and *hcar* Arabidopsis proto-plasts (Supplementary Fig. 16), indicating that like Pheo *a* and RCC, 7-HMC *a* also acts as a photosensitizer *in vivo*.

High levels of Pheo *a* accumulate in *athcar* plants during dark incubation (Meguro et al., 2011). We therefore investigated whether Pheo *a* also accumulates in the *oshcar* mutant. Before dark incubation, Pheo *a* was barely detected in wild-type and *oshcar* leaves. After 4 DDI, however, high levels of Pheo *a* accumulated in *hcar* leaves (Figs. 9A and 9B). We also investigated whether the levels of *PAO* mRNA and/or PAO protein are related to Pheo *a* accumulation in *oshcar* leaves. By RT-qPCR analysis, we found that the mRNA level of *PAO* in *oshcar* leaves was not significantly different to that of wild-type leaves (Fig. 9C), like the expression patterns of other CCE genes, such as *SGR1*, *NYC1*, *NOL*, *PPH*, and *RCCR* (Supplementary Fig. 17). Like the mRNA level, the protein level of PAO in the *oshcar* leaves was also similar to that of wild-type leaves (Fig. 9D), indicating that Pheo *a* accumulation in *oshcar* leaves is caused by an unknown mechanism independent of PAO protein level.

DISCUSSION

Rice HCAR is a functional homolog of Arabidopsis HCAR involved in Chl breakdown

AtHCAR is a key enzyme in the PAO/phyllobilin pathway for Chl degradation; it catalyzes the conversion of 7-HMC *a* to Chl *a in vivo* and *in vitro*, and the *athcar* mutant shows a stay-green phenotype during DIS (Meguro et al., 2011). In this study, we found that, like the *athcar* mutant, the *oshcar* mutant exhibits persistent leaf greenness much longer than wild type during DIS and natural senescence (Fig. 1; Supplementary Fig. 2), along with the accumulation of 7-HMC *a* and Pheo *a* (Fig. 2). Furthermore, overexpressing *OsHCAR* recovered the defects of the *athcar* mutant (Supplementary Fig. 4), strongly indicating that *OsHCAR* is a functional homolog of *AtHCAR*.

In Arabidopsis, HCAR interacts with other CCEs, such as SGR1/NYE1, NYC1, NOL, and RCCR, during leaf senescence (Sakuraba et al., 2013). Similarly, in rice, OsHCAR also interacted with SGR, NYC1, and NOL in yeast two-hybrid assays (Fig. 3). Interestingly, we also found that OsHCAR interacted with itself (Fig. 3), suggesting that OsHCAR can form homo-dimers or -trimers. The importance of the HCAR-HCAR interaction remains unclear. Very recently, Wang and Liu (2016) determined the crystal structure of AtHCAR and found that it has the potential to form trimers, which is likely important for its interaction with LHCII. Similarly, we previously showed that Arabidopsis SGR1/NYE1 forms a homo-dimer and/or hetero-dimer with other SGR homologs in Arabidopsis, i.e., SGR2 and SGR-LIKE (SGRL), possibly to help control the rate of Chl degradation (Sakuraba et al., 2014b; 2014c). In this respect, HCAR dimer (or trimer) formation is probably important for enhancing its functions, e.g., its interaction capacity with LHCII and other CCEs, similar to SGR/Mg-dechelatase proteins.

Although the physiological role of OsHCAR is almost

equivalent to that of AtHCAR, we found that the mRNA expression pattern of *OsHCAR* considerably differs from that of *AtHCAR*. Similar to *AtNOL* (Sakuraba et al., 2013), *AtHCAR* expression decreased during DIS, while the expression of *OsHCAR* and *OsNOL* increased under both DIS and natural senescence (Fig. 4). These results strongly suggest that the requirement for HCAR and NOL activity somehow differs in Arabidopsis and rice, especially in chloroplasts at the senescence phase. Indeed, the phenotypes of Arabidopsis and rice *nol* null mutants are quite different during leaf senescence: the rice *nol* plants display a stay-green phenotype (Sato et al., 2009), whereas the Arabidopsis *nol* plants undergo normal yellowing (Horie et al., 2009). Similarly, the *oshcar* mutant showed a strong stay-green phenotype during natural senescence in the paddy field (Supplementary Fig. 2), whereas the *athcar* mutant did not exhibit a stay-green phenotype during natural senescence, although both mutants remained green under DIS conditions (Fig. 1; Sakuraba et al., 2013). The different patterns of *HCAR* and *NOL* expression between Arabidopsis and rice further confirm that the transcriptional regulatory networks of these two genes are quite dissimilar. In Arabidopsis, several transcription factors, such as ABI5/EEL, ORE1, EIN3, ANAC016, and ANAC072, directly activate the transcription of CCE genes, including *SGR1/NYE1* (Li et al., 2016; Qiu et al., 2015; Sakuraba et al., 2014a; 2016), and a few directly activate more than two CCE genes. For example, EIN3 and ORE1 directly activate the transcription of *SGR1/NYE1*, *NYC1*, and *PAO* (Qiu et al., 2015); this co-activation is likely important because these genes function during the same phase. However, the expression patterns of *AtHCAR* and *AtNOL* suggest that these genes are regulated by transcription factors in different regulatory networks. In rice, two NAC TFs, OsNAP, and ONAC106, directly regulate the expression of CCEs, including *SGR*. OsNAP directly activates the transcription of *SGR*, *NYC1*, *NYC3/PPH*, and *RCCR*, whereas ONAC106 directly downregulates the expression of *SGR* and *NYC1* during leaf senescence (Sakuraba et al., 2015b). The induction of CCE co-expression by a single transcription factor in rice suggests that *HCAR* and *NOL* are co-expressed with other CCEs by transcription factors in the same regulatory network. The upstream regulatory network of *HCAR* and *NOL* must be identified in both Arabidopsis and rice to evaluate the importance of the differential expression patterns of these genes in these plants.

HCAR plays an important role in preventing cell death signaling in rice and Arabidopsis

Under high-light conditions, Chl and its intermediates produce high levels of singlet oxygen, because their excited forms react with triplet oxygen, leading to the production of the highly reactive oxygen species $^1O_2$. Protoporphyrin IX (Proto IX) and protochlorophyllide (Pchlide) are strong photosensitizers in the Chl biosynthesis pathway (Jung et al., 2008; Nagata et al., 2005; op den Camp et al., 2003), whereas Pheo *a* and RCC are strong photosensitizers in the Chl degradation pathway: Arabidopsis *pao* and *rccr* mutants, also known as *acd1* and *acd2*, respectively, show severe cell death symptoms, accompanied by the production of singlet

oxygen (Pružinská et al., 2007). However, it was previously unclear whether other Chl intermediates can also have photo-toxic effects.

In this study, we found that the *oshcar* mutant suffered from cell death symptoms in mature leaves under normal growth conditions in both the paddy field and growth chamber. We also found that *oshcar* mutant is also susceptible to herbicide-induced oxidative stress conditions (Fig. 5), and similar cell death symptoms in the Arabidopsis *hcar* mutant was also observed (Fig. 6). It has been known that MV blocks the electron transport during photosynthesis in the chloroplasts, leading to the production of $^1O_2$. Produced $^1O_2$ indirectly promotes the degradation of Chls, as well as photosystem apparatus, and further $^1O_2$ is produced by the accumulation of 7-HMC *a* and Pheo *a* in *hcar* mutants, similar to *rccr* mutant (Yao and Greenberg, 2006). Furthermore, both rice and Arabidopsis protoplasts incubated with purified 7-HMC *a* produced large amounts of singlet oxygen (Fig. 8; Supplementary Fig. 13), indicating that 7-HMC *a* also acts as a phototoxic molecule. Pheo *a* also accumulates in *hcar* mutants, especially during DIS and under oxidative stress (Fig. 8; Meguro et al., 2011). Thus, the cell death phenotype of the *hcar* mutants is probably caused by the accumulation of both 7-HMC *a* and Pheo *a*. Like 7-HMC *a* and Pheo *a*, some Chl catabolic intermediates have the potential to act as phototoxic molecules. Both rice and Arabidopsis HCAR physically interact with other CCEs to form the Chl degradation complex at LHCII (Fig. 3; Sakuraba et al., 2013; 2015a); this complex formation is likely important for preventing the escape of such Chl catabolic intermediates from chloroplasts into the cytoplasm.

It is also possible that excessive accumulation of 7-HMC *a* changes the pigment composition in Chl-containing photosystem proteins in non-senescent green leaves. Indeed, in transgenic Arabidopsis plants overexpressing chlorophyllide *a* oxygenase (*CAO*-OX), high levels of Chl *b* accumulate in leaves, leading to changes in Chl *a/b* ratios in Chl-binding photosystem proteins, including LHCII and the subunits of core complexes (Sakuraba et al., 2009; Yamasato et al., 2005). Furthermore, *CAO*-OX plants exhibit cell death symptoms under high-light conditions, because their altered Chl composition ultimately changes their energy transfer capacity (Sakuraba et al., 2010), indicating that maintaining the proper balance of Chl composition in photosystem complexes is important for preventing cell death due to excessive light damage. Similarly, it is highly likely that the excessive 7-HMC *a* in the *hcar* mutants enters into the binding sites of Chls instead of photosystem proteins, leading to severe cell death symptoms (Figs. 5-7). Further biochemical studies, such as studies examining the Chl composition of photosystem proteins in *hcar* mutants, are needed to explore these possibilities.

Gene information Sequence data from this article can be found in the National Center for Biotechnology Information (NCBI) database under the following accession numbers: for Arabidopsis, *AtHCAR*, At1g04620; for rice, *GAPDH*, Os06g45590; *JAmyb*, Os11g0684000; *MT2b*, Os05g0111300; *NOL*, Os03g0654600; *NYC1*, Os01g0227100; *OsACS6*, Os02g

49880; *OsHCAR*, Os04g0320100; *OsNAC4*, Os01g60020; *PAO*, Os03g0146400; *PPH*, Os06g0354700; *RCCR*, Os10g0389200; *SGR*, Os09g0532000; *SGRL*, Os04g0692600; *UBQ5*, Os01g0328400.

Note: Supplementary information is available on the Molecules and Cells website (www.molcells.org).

REFERENCES

Barry, C.S., McQuinn, R.P., Chung, M.Y., Besuden, A., and Giovannoni, J.J. (2008). Amino acid substitutions in homologs of the STAY-GREEN protein are responsible for the green-flesh and chlorophyll retainer mutations of tomato and pepper. Plant Physiol. *147*, 179-187.

Greenberg, J.T., Guo, A., Klessig, D.F., and Ausubel, F.M. (1994). Programmed cell death in plants: a pathogen-triggered response activated coordinately with multiple defense functions. Cell *77*, 551-563.

Han, S.H., Sakuraba, Y., Koh, H.J., and Paek, N.C. (2012). Leaf variegation in the rice zebra2 mutant is caused by photoperiodic accumulation of tetra-cis-lycopene and singlet oxygen. Mol. Cells *33*, 87-97.

Horie, Y., Ito, H., Kusaba, M., Tanaka, R., and Tanaka, A. (2009). Participation of chlorophyll b reductase in the initial step of the degradation of light-harvesting chlorophyll a/b-protein complexes in Arabidopsis. J. Biol. Chem. *284*, 17449-17456.

Hörtensteiner, S. (2009). Stay-green regulates chlorophyll and chlorophyll-binding protein degradation during senescence. Trends Plant Sci. *14*, 155-162.

Hörtensteiner, S. (2013). Update on the biochemistry of chlorophyll breakdown. Plant Mol. Biol. *82*, 505-517.

Hörtensteiner, S., and Krautler, B. (2011). Chlorophyll breakdown in higher plants. Biochim. Biophys. Acta *1807*, 977-988.

Ito, H., Yokono, M., Tanaka, R., and Tanaka, A. (2008). Identification of a novel vinyl reductase gene essential for the biosynthesis of monovinyl chlorophyll in Synechocystis sp. PCC6803. J. Biol. Chem. *283*, 9002-9011.

Jeon, J.S., Lee, S., Jung, K.H., Jun, S.H., Jeong, D.H., Lee, J., Kim, C., Jang, S., Yang, K., Nam, J., et al. (2000). T-DNA insertional mutagenesis for functional genomics in rice. Plant J. *22*, 561-570.

Jung, S., Lee, H.J., Lee, Y., Kang, K., Kim, Y.S., Grimm, B., and Back, K. (2008). Toxic tetrapyrrole accumulation in protoporphyrinogen IX oxidase-overexpressing transgenic rice plants. Plant Mol, Biol, *67*, 535-546,

Koch, E., and Slusarenko, A. (1990). Arabidopsis is susceptible to infection by a downy mildew fungus. Plant Cell *2*, 437-445.

Kusaba, M., Ito, H., Morita, R., Iida, S., Sato, Y., Fujimoto, M., Kawasaki, S., Tanaka, R., Hirochika, H., Nishimura, M., et al. (2007). Rice NON-YELLOW COLORING1 is involved in light-harvesting complex II and grana degradation during leaf senescence. Plant Cell

19, 1362-1375.

Li, J., Pandeya, D., Nath, K., Zulfugarov, I.S., Yoo, S.C., Zhang, H., Yoo, J.H., Cho, S.H., Koh, H.J., Kim, D.S., et al. (2010). ZEBRA-NECROSIS, a thylakoid-bound protein, is critical for the photoprotection of developing chloroplasts during early leaf development. Plant J. 62, 713-725.

Li, S., Gao, J., Yao, L., Ren, G., Zhu, X., Gao, S., Qiu, K., Zhou, X., and Kuai, B. (2016). The role of ANAC072 in the regulation of chlorophyll degradation during age- and dark-induced leaf senescence. Plant Cell Rep. 35, 1729-1741.

Liang, H., Yao, N., Song, J.T., Luo, S., Lu, H., and Greenberg, J.T. (2003). Ceramides modulate programmed cell death in plants. Genes Dev. 17, 2636-2641.

Liang, C., Wang, Y., Zhu, Y., Tang, J., Hu, B., Liu, L., Ou, S., Wu, H., and Chu, C. (2014). OsNAP connects abscisic acid and leaf senescence by fine-tuning abscisic acid biosynthesis and directly targeting senescence-associated genes in rice. Proc. Natl. Acad. Sci. USA 111, 10013-10018.

Livak, K.J., and Schmittgen, T.D. (2001). Analysis of relative gene expression data using real-time quantitative PCR and the 2(-Delta Delta C(T)) Method. Methods 25, 402-408.

Meguro, M., Ito, H., Takabayashi, A., Tanaka, R., and Tanaka, A. (2011). Identification of the 7-hydroxymethyl chlorophyll a reductase of the chlorophyll cycle in Arabidopsis. Plant Cell 23, 3442-3453.

Nagata, N., Tanaka, R., Satoh, S., and Tanaka, A. (2005). Identification of a vinyl reductase gene for chlorophyll synthesis in Arabidopsis thaliana and implications for the evolution of Prochlorococcus species. Plant Cell 17, 233-240.

op den Camp, R.G., Przybyla, D., Ochsenbein, C., Laloi, C., Kim, C., Danon, A., Wagner, D., Hideg, E., Gobel, C., Feussner, I., et al. (2003). Rapid induction of distinct stress responses after the release of singlet oxygen in Arabidopsis. Plant Cell 15, 2320-2332.

Park, S.Y., Yu, J.W., Park, J.S., Li, J., Yoo, S.C., Lee, N.Y., Lee, S.K., Jeong, S.W., Seo, H.S., Koh, H.J., et al. (2007) The senescence-induced staygreen protein regulates chlorophyll degradation. Plant Cell 19, 1649-1664.

Porra, R.J., Thompson, W.A., and Kriedemann, P.E. (1989). Determination of accurate extinction coefficients and simultaneous equations for assaying chlorophylls a and b extracted with four different solvents: verification of the concentration of chlorophyll standards by atomic absorption spectrometry. Biochim. Biophys. Acta 975, 384-394.

Pružinská, A., Tanner, G., Anders, I., Roca, M., and Hörtensteiner, S. (2003) Chlorophyll breakdown: pheophorbide a oxygenase is a Rieske-type iron-sulfur protein, encoded by the accelerated cell death 1 gene. Proc, Natl, Acad, Sci, USA 100, 15259-15264.

Pružinská, A., Anders, I., Aubry, S., Schenk, N., Tapernoux-Luthi, E., Muller, T., Krautler, B., and Hörtensteiner, S. (2007) In vivo participation of red chlorophyll catabolite reductase in chlorophyll breakdown. Plant Cell 19, 369-387.

Qiu, K., Li, Z., Yang, Z., Chen, J., Wu, S., Zhu, X., Gao, S., Gao, J., Ren, G., Kuai, B., et al. (2015). EIN3 and ORE1 accelerate degreening during ethylene-mediated leaf senescence by directly activating chlorophyll catabolic genes in Arabidopsis. PLoS Genet. 11, e1005399.

Ren, G., An, K., Liao, Y., Zhou, X., Cao, Y., Zhao, H., Ge, X., and Kuai, B. (2007). Identification of a novel chloroplast protein AtNYE1 regulating chlorophyll degradation during leaf senescence in Arabidopsis. Plant Physiol. 144, 1429-1441.

Rong, H., Tang, Y., Zhang, H., Wu, P., Chen, Y., Li, M., Wu, G., and Jiang, H. (2013). The Stay-Green Rice like (SGRL) gene regulates chlorophyll degradation in rice. J. Plant Physiol. 170, 1367-1373.

Sakuraba, Y., Tanaka, R., Yamasato, A., and Tanaka, A. (2009). Determination of a chloroplast degron in the regulatory domain of chlorophyllide a oxygenase. J. Biol. Chem. 284, 36689-36699.

Sakuraba, Y., Yokono, M., Akimoto, S., Tanaka, R., and Tanaka, A. (2010). Deregulated chlorophyll b synthesis reduces the energy transfer rate between photosynthetic pigments and induces photodamage in Arabidopsis thaliana. Plant Cell Physiol. 51, 1055-1065.

Sakuraba, Y., Schelbert, S., Park, S.Y., Han, S.H., Lee, B.D., Andres, C.B., Kessler, F., Hörtensteiner, S., and Paek, N.C. (2012). STAY-GREEN and chlorophyll catabolic enzymes interact at light-harvesting complex II for chlorophyll detoxification during leaf senescence in Arabidopsis. Plant Cell 24, 507-518.

Sakuraba, Y., Kim, Y.S., Yoo, S.C., Hörtensteiner, S., and Paek, N.C. (2013). 7-Hydroxymethyl chlorophyll a reductase functions in metabolic channeling of chlorophyll breakdown intermediates during leaf senescence. Biochem. Biophys. Res. Commun. 430, 32-37.

Sakuraba, Y., Jeong, J., Kang, M.Y., Kim, J., Paek, N.C., and Choi, G. (2014a). Phytochrome-interacting transcription factors PIF4 and PIF5 induce leaf senescence in Arabidopsis. Nat. Commun. 5, 4636.

Sakuraba, Y., Kim, D., Kim, Y.S., Hörtensteiner, S., and Paek, N.C. (2014b). Arabidopsis STAYGREEN-LIKE (SGRL) promotes abiotic stress-induced leaf yellowing during vegetative growth. FEBS Lett. 588, 3830-3837.

Sakuraba, Y., Park, S.Y., Kim, Y.S., Wang, S.H., Yoo, S.C., Hörtensteiner, S., and Paek, N.C. (2014c). Arabidopsis STAY-GREEN2 is a negative regulator of chlorophyll degradation during leaf senescence. Mol. Plant 7, 1288-1302.

Sakuraba, Y., Park, S.Y., and Paek, N.C. (2015a) The divergent roles of STAYGREEN (SGR) homologs in chlorophyll degradation. Mol Cells 38, 390-395.

Sakuraba, Y., Piao W., Lim J.H., Han S.H., Kim Y.S., An G., and Paek N.C. (2015b). Rice ONAC106 inhibits leaf senescence and increases salt tolerance and tiller angle. Plant Cell Physiol. 56, 2325-2339.

Sakuraba, Y., Han, S.H., Lee, S.H., Hörtensteiner, S., and Paek, N.C. (2016). Arabidopsis NAC016 promotes chlorophyll breakdown by directly upregulating STAYGREEN1 transcription. Plant Cell Rep. 35, 155-166.

Sato, Y., Morita, R., Katsuma, S., Nishimura, M., Tanaka, A., and Kusaba, M. (2009). Two short-chain dehydrogenase/reductases, NON-YELLOW COLORING 1 and NYC1-LIKE, are required for chlorophyll b and light-harvesting complex II degradation during senescence in rice. Plant J. 57, 120-131.

Schelbert, S., Aubry, S., Burla, B., Agne, B., Kessler, F., Krupinska, K., and Hörtensteiner, S. (2009) Pheophytin pheophorbide hydrolase (pheophytinase) is involved in chlorophyll breakdown during leaf senescence in Arabidopsis. Plant Cell 21, 767-785.

Shimoda, Y., Ito, H., and Tanaka, A. (2016). Arabidopsis STAY-GREEN, Mendel's green cotyledon gene, encodes magnesium-dechelatase. Palnt Cell 28, 2147-2160.

Tang, Y., Li, M., Chen, Y., Wu, P., Wu, G., and Jiang, H. (2011). Knockdown of OsPAO and OsRCCR1 cause different plant death phenotypes in rice. J. Plant Physiol. 168, 1952-1959.

Wang, S.H., Lim, J.H., Kim, S.S., Cho, S.H., Yoo, S.C., Koh, H.J., Sakuraba, Y., and Paek, N.C. (2015) Mutation of SPOTTED LEAF3 (SPL3) impairs abscisic acid-responsive signalling and delays leaf senescence in rice. J. Exp. Bot. 66, 7045-7059.

Wang, X., and Liu, L. (2016) Crystal structure and catalytic mechanism of 7-hydroxymethyl chlorophyll a reductase. J. Biol. Chem. 291, 13349-13359.

Yamasato, A., Nagata, N., Tanaka, R., and Tanaka, A. (2005). The N-

terminal domain of chlorophyllide a oxygenase confers protein instability in response to chlorophyll B accumulation in Arabidopsis. Plant Cell *17,* 1585-1597.

Yao, N., and Greenberg, J.T. (2006). Arabidopsis ACCELERATED CELL DEATH2 modulates programmed cell death. Plant Cell *18,* 397-411.

Wu, F.H., Shen, S.C., Lee, L.Y., Chan, M.T., and Lin, C.S. (2009). Tape-Arabidopsis Sandwich- a simpler Arabidopsis protoplast isolation method. Plant Methods *5,* 16.

Zapata, M., Rodriguez, F., and Garrido, J.L. (2000). Separation of chlorophylls and carotenoids from marine phytoplankton: a new HPLC method using a reversed phase C8 column and pyridine-containing mobile phases. Mar. Ecol. Prog. Ser. *195,* 29-45.

Zhang, X., Henriques, R., Lin, S.S., Niu, Q.W., and Chua, N.H. (2006). Agrobacterium-mediated transformation of Arabidopsis thaliana using the floral dip method. Nat. Protoc. *1,* 641-646.